Article

Amine Basicity (p*K*) Controls the Analyte Binding Energy on Single Walled Carbon Nanotube Electronic Sensor Arrays

Chang Young Lee, and Michael S. Strano

J. Am. Chem. Soc., **2008**, 130 (5), 1766-1773 • DOI: 10.1021/ja0776069

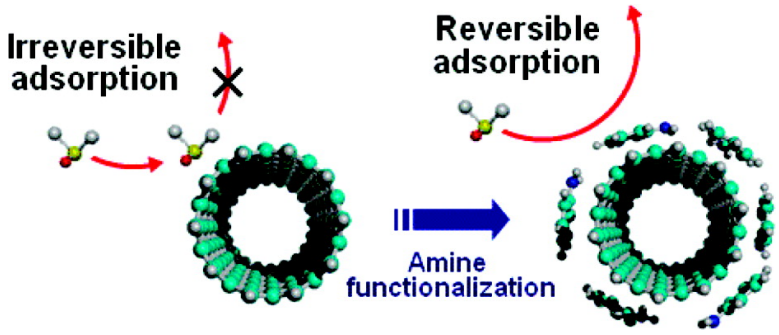

More About This Article

Additional resources and features associated with this article are available within the HTML version:

- Supporting Information
- Links to the 4 articles that cite this article, as of the time of this article download
- Access to high resolution figures
- Links to articles and content related to this article
- Copyright permission to reproduce figures and/or text from this article

View the Full Text HTML

J|A|C|S
ARTICLES
Published on Web 01/12/2008

Amine Basicity (pK_b) Controls the Analyte Binding Energy on Single Walled Carbon Nanotube Electronic Sensor Arrays

Chang Young Lee and Michael S. Strano*

Department of Chemical Engineering, Massachusetts Institute of Technology, Cambridge, Massachusetts 02139

Received October 2, 2007; E-mail: strano@mit.edu

Abstract: A wide range of analytes adsorb irreversibly to the surfaces of single walled carbon nanotube electronic networks typically used as sensors or thin-film transistors, although to date, the mechanism is not understood. Using thionyl chloride as a model electron-withdrawing adsorbate, we show that reversible adsorption sites can be created on the nanotube array via noncovalent functionalization with amine-terminated molecules of pK_a < 8.8. A nanotube network comprising single, largely unbundled nanotubes, near the electronic percolation threshold is required for the effective conversion to a reversibly binding array. By examining 11 types of amine-containing molecules, we show that analyte adsorption is largely affected by the basicity (pK_b) of surface groups. The binding energy of the analyte is apparently reduced by its adsorption on the surface chemical groups instead of directly on the SWNT array itself. This mediated adsorption mechanism is supported by X-ray photoelectron spectroscopy (XPS) and molecular potential calculations. Reversible detection with no active regeneration at the parts-per-trillion level is demonstrated for the first time by creating a higher adsorption site density with a polymer amine, such as polyethyleneimine (PEI). Last, we demonstrate that this transition to reversibility upon surface functionalization is a general phenomenon.

1. Introduction

Single walled carbon nanotubes (SWNT) are unique adsorbents with high surface to volume ratio and all atoms residing on the surface. The one-dimensional electronic structure of SWNT is readily disrupted by single adsorption events.[1,2] Hence, sorption-based sensors from these materials have become a promising application.[3] Although recent studies by Snow et al.[4,5] have utilized a capacitor arrangement, most nanotube sensors operate as chemiresistors, where the conductance change upon molecular adsorption to the nanotube sidewall is monitored. Sensitivity and selectivity have been enhanced by applying selective binding ligands such as polymers,[6] DNA,[7] or metal nanoparticles.[8] Oxidation defects apparently increase sensitivity as well.[9] The sensitivity of SWNT gas sensors scales with the exposed surface area[10] and typically reaches the ppb level for several systems in the literature.[6,11] The typically cited mechanism for the electrical response is the adsorption-induced change in nanotube Fermi level and density of electronic states.[3] The role of the SWNT-electrode contact has been studied by contact-passivation, showing discrepant results to date.[10,12,13]

The nature of molecular adsorption onto SWNT remains poorly understood in several respects. Strong electron donors or acceptors appear to adsorb onto single nanotube or network devices irreversibly at temperatures near ambient. Consequently, the majority of SWNT gas sensors reported to date have an irreversible component in their responses.[4,6,8,10−12,14,15] We define reversible or partially reversible sensors as those that restore 50% of the initial baseline within 60 s of analyte removal (halfway recovery time $t_{1/2}$ < 60 s). The remainders are defined as irreversible sensors. While seemingly arbitrary, this classification is unambiguous and lends itself to a compelling molecular description, as described below. Examples of these types of irreversible electrical responses are shown in Figure 1 for a number of analytes from many different research groups and sensor configurations. Subsequent data from the same systems occasionally demonstrate reversible sensor responses

(1) Peng, S.; Cho, K. J.; Qi, P. F.; Dai, H. J. *Chem. Phys. Lett.* **2004**, *387*, 271−276.
(2) Tournus, F.; Latil, S.; Heggie, M. I.; Charlier, J. C. *Phys. Rev. B* **2005**, *72*, 075431.
(3) Kong, J.; Franklin, N. R.; Zhou, C. W.; Chapline, M. G.; Peng, S.; Cho, K. J.; Dai, H. J. *Science* **2000**, *287*, 622−625.
(4) Snow, E. S.; Perkins, F. K.; Houser, E. J.; Badescu, S. C.; Reinecke, T. L. *Science* **2005**, *307*, 1942−1945.
(5) Snow, E. S.; Perkins, F. K. *Nano Lett.* **2005**, *5*, 2414−2417.
(6) Qi, P.; Vermesh, O.; Grecu, M.; Javey, A.; Wang, O.; Dai, H. J.; Peng, S.; Cho, K. J. *Nano Lett.* **2003**, *3*, 347−351.
(7) Staii, C.; Johnson, A. T. *Nano Lett.* **2005**, *5*, 1774−1778.
(8) Lu, Y. J.; Li, J.; Han, J.; Ng, H. T.; Binder, C.; Partridge, C.; Meyyappan, M. *Chem. Phys. Lett.* **2004**, *391*, 344−348.
(9) Robinson, J. A.; Snow, E. S.; Badescu, S. C.; Reinecke, T. L.; Perkins, F. K. *Nano Lett.* **2006**, *6*, 1747−1751.
(10) Lee, C. Y.; Baik, S.; Zhang, J. Q.; Masel, R. I.; Strano, M. S. *J. Phys. Chem.* B **2006**, *110*, 11055−11061.
(11) Novak, J. P.; Snow, E. S.; Houser, E. J.; Park, D.; Stepnowski, J. L.; McGill, R. A. *Appl. Phys. Lett.* **2003**, *83*, 4026−4028.
(12) Bradley, K.; Gabriel, J. C. P.; Star, A.; Gruner, G. *Appl. Phys. Lett.* **2003**, *83*, 3821−3823.
(13) Zhang, J.; Boyd, A.; Tselev, A.; Paranjape, M.; Barbara, P. *Appl. Phys. Lett.* **2006**, *88*, 123112.
(14) Bekyarova, E.; Davis, M.; Burch, T.; Itkis, M. E.; Zhao, B.; Sunshine, S.; Haddon, R. C. *J. Phys. Chem. B* **2004**, *108*, 19717−19720.
(15) Nguyen, H. Q.; Huh, J. S. *Sens. Actuators, B* **2006**, *117*, 426−430.
(16) Cattanach, K.; Kulkarni, R. D.; Kozlov, M.; Manohar, S. K. *Nanotechnology* **2006**, *17*, 4123−4128.
(17) Zhang, T.; Nix, M. B.; Yoo, B. Y.; Deshusses, M. A.; Myung, N. V. *Electroanal.* **2006**, *18*, 1153−1158.

10.1021/ja0776069 CCC: $40.75

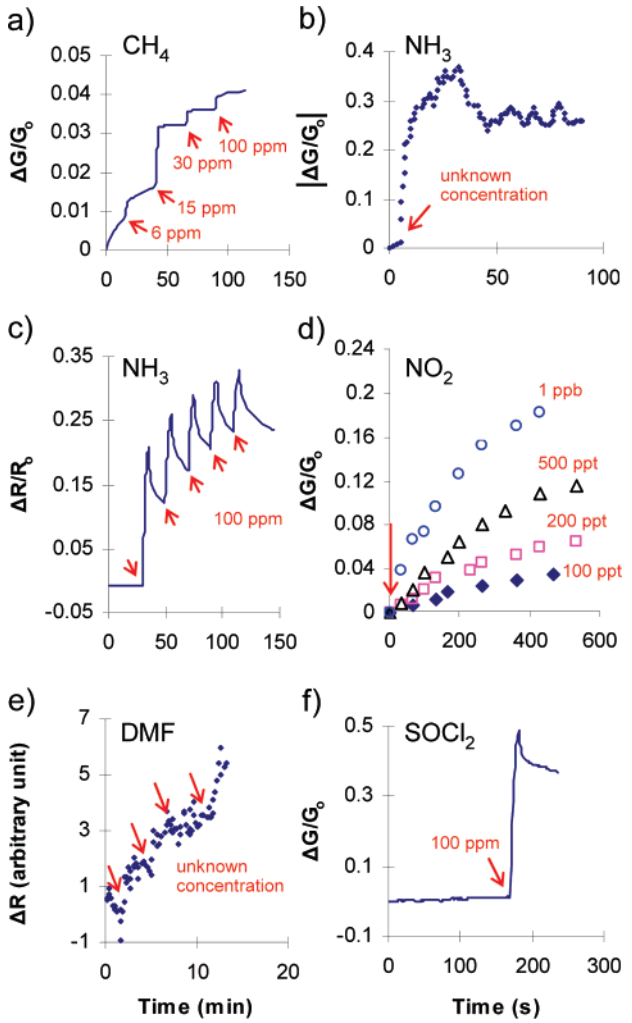

Figure 1. Examples of irreversible sensor responses of various analytes onto a number of single walled carbon nanotube arrays described in previous reports. We have defined that irreversible sensors do not restore 50% of the baseline within 60 s of analyte removal ($t_{1/2}$ > 60 s). The majority of systems published to date show irreversible conductance (G) or resistance (R) changes upon exposure to analytes due to a yet unexplained mechanism. (a) CH_4 responses from Lu et al.[8] (b) NH_3 response from Novak et al.[11] (c) NH_3 responses from Bekyarova et al.[14] (d) NO_2 responses from Qi et al.[6] (e) dimethylformamide (DMF) responses from Snow et al.[4] (f) $SOCl_2$ response from Lee et al.[10]

for the same analytes;[5,7,16,17] however this contradictory behavior is not acknowledged or discussed in previous reports. Incidentally, such systems are typically regenerated manually and therefore slowly, using methods including UV irradiation,[18] annealing,[3] applying electric fields,[11] and hydrolysis of analytes.[10] Our previous work clearly identifies the irreversible electrical response as arising from irreversible molecular adsorption of the analyte.[10]

The transition between irreversible and reversible binding to a nanotube surface is a direct probe of the energetics of the adsorption process. The equilibrium constant of adsorption, obtainable directly from the transient sensor response, includes both entropic and enthalpic factors. A great number of mechanisms influence the thermodynamics of binding to these systems, including electron donor/acceptor interactions, dipole-induced dipole interactions, and steric influences of nanoscale curvature. Nanotube bundles, with spaces formed between neighboring nanotubes, form high-energy pores of various potential. Last, junctions between metal and semiconducting SWNT possess uniqueness in both geometric and electronic properties.

In this work, we demonstrate, for the first time, the controlled tuning of adsorption energies on single walled carbon nanotube arrays, separating the influences of steric and electronic factors controlling the free energy of adsorption. Dielectrophoresis is utilized to generate SWNT electronic networks both above and below the percolation transition. Using thionyl chloride as a model adsorbate, the adsorption response is tuned by chemically treating the array with n-doping amines of pK_a < 8.8. The free energy of adsorption, extracted from reversible responses, is comparable to simple molecular potential (MP) calculation results. In situ conductance and simultaneous Raman measurements were performed to find conditions for effective amine functionalization. A mechanism for tuning reversibility is proposed based on in situ Raman, X-ray photoelectron spectroscopy (XPS), and MP calculations. Understanding the science of molecular adsorption enables us to reversibly detect the analyte with significantly enhanced sensitivity via polymer-functionalization.

2. Results and Discussion

Dielectrophoresis of an aqueous solution of SWNT and surfactant between 5 μm Au electrodes produces networks of varying connectivity and bundle size nearly a monolayer thin. As-produced SWNT networks show a stepwise conductance increase upon a pulsed 10 mL injection of 1 ppm thionyl chloride (Figure 2a). The signal does not restore to the baseline value for several days. This type of response is typical and well documented for these systems by our laboratory and others.[8,10,14] In the case of thionyl chloride, it was conclusively demonstrated using subsequent hydrolysis that irreversible adsorption is responsible for the persistence of the response.[10] Thionyl chloride is a strong electron acceptor. The conductance increase is due to the enrichment of hole carriers by p-doping or enhanced electron transmission through nanotube−nanotube or nanotube−electrode contacts.

In this paper, however, we find that this behavior is altered when the array is noncovalently functionalized by dropping and evaporating either small or large molecular weight amine-bearing molecules such as pyridine, aniline, hydrazine, and ethylenediamine. The current decreases immediately upon amine functionalization, consistent with n-doping by lone pair electrons.[6] The sensor responses after amine-functionalization become reversible as in Figures 2b−e. Negligible drift in the baseline is observed after subsequent exposures. We have found that this irreversible-to-reversible transition is general for a wide range of analyte concentrations. Adsorption (k) and desorption (k_{-1}) rate constants, and thus the equilibrium constant (K) for thionyl chloride adsorption can be extracted using our previously developed model.[19]

$$S(t) = S_o \exp[-k_{-1}t] \quad (1)$$

$$S(t) = S_{max}\frac{C_aK}{1+C_aK}\left(1-\exp\left[-\frac{1+C_aK}{K}kt\right]\right) \quad (2)$$

(18) Chen, R. J.; Franklin, N. R.; Kong, J.; Cao, J.; Tombler, T. W.; Zhang, Y. G.; Dai, H. J. *Appl. Phys. Lett.* **2001**, *79*, 2258−2260.

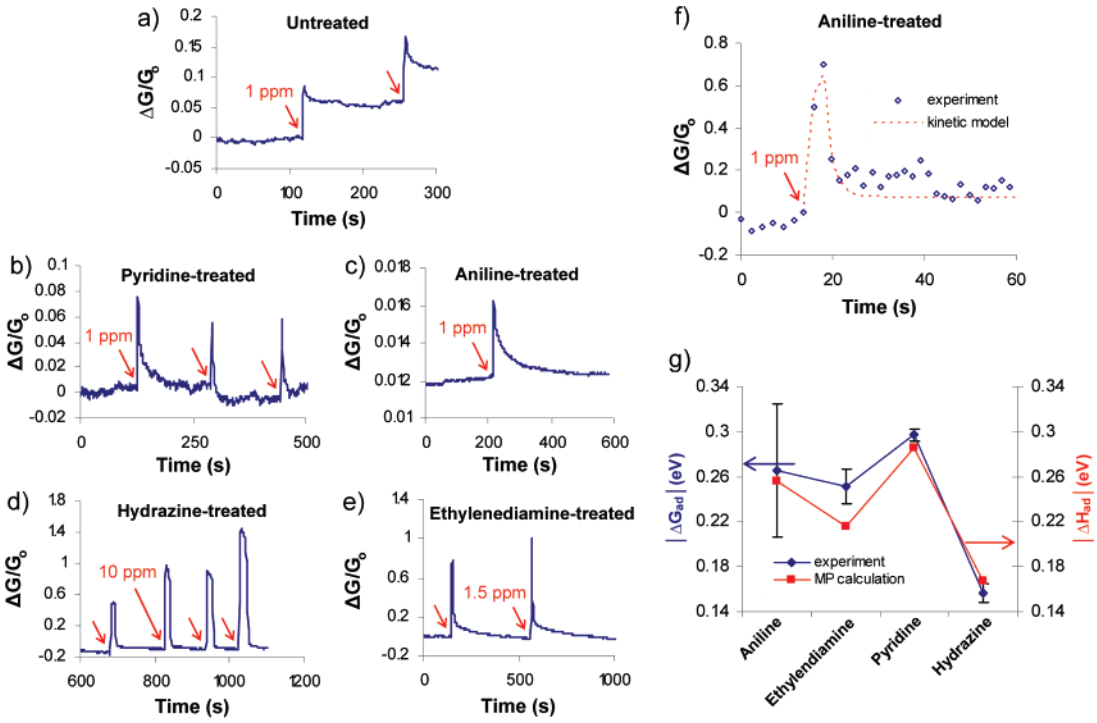

Figure 2. Tuning the sensor reversibility by surface chemistry. Normalized conductance change ($\Delta G/G_o$) was monitored upon exposure to thionyl chloride. (a) Irreversible stepwise signal increase from untreated sensor. Reversible responses from sensors treated with pyridine (b), aniline (c), hydrazine (d), and ethylenediamine (e). The phenomenon is reproducibly observed for various analyte concentrations. (f) A reversible response (diamond) fitted using our kinetic model (dotted line). (g) Comparison between the extracted free energy from experiment (diamond) and adsorption enthalpy from MP calculation (square).

Table 1. Kinetic and Thermodynamic Parameters of Thionyl Chloride Adsorption for 4 Amine-functionalizations[a]

functionalization	k_{-1} (s^{-1})	k ($ppb^{-1}\ s^{-1}$)	K (ppb^{-1})	ΔG_{ad} (eV)	$\Delta H_{ad,MP}$ (eV)
aniline	0.21 ± 0.23	$(0.60 \pm 4.99) \times 10^{-5}$	$(2.8 \pm 9.7) \times 10^{-5}$	-0.27 ± 0.06	-0.256
ethylenediamine	0.62 ± 0.26	$(1.0 \pm 0.5) \times 10^{-5}$	$(1.7 \pm 1.0) \times 10^{-5}$	-0.25 ± 0.02	-0.216
pyridine	0.17 ± 0.05	$(1.6 \pm 0.6) \times 10^{-5}$	$(9.5 \pm 1.8) \times 10^{-5}$	$-0.30 \pm 0.00_5$	-0.285
hydrazine	0.10 ± 0.05	$(4.1 \pm 3.5) \times 10^{-8}$	$(4.2 \pm 1.5) \times 10^{-7}$	-0.16 ± 0.01	-0.167

[a] Sensor responses were fitted to eqs 1−3 to extract all the values except for $\Delta H_{ad,MP}$, which was obtained via molecular potential (MP) calculation.

S and C_a denote the sensor signal ($\Delta G/G_o$) and analyte concentration, respectively. From the earlier definition of reversibility and $t_{1/2} = (1/k_{-1})\ln 2$ from eq 1, $k_{-1} > 1.16 \times 10^{-2}$ s^{-1} is expected for reversible sensors. Extracting kinetic/thermodynamic parameters by fitting the reversible response is shown using the aniline-treated sensor as an example (Figure 2f).[20] The desorption part, an exponential decay from the signal when analyte is removed (S_o), is fitted to eq 1 to determine $k_{-1} = 0.51\ s^{-1}$. Maximum signal (S_{max}) upon saturation of the sensor surface was estimated to be around 2.71 by exposing the sensor to excess amount of saturated thionyl chloride vapor. Values for $k = 1.7 \times 10^{-4}\ ppb^{-1}s^{-1}$ and $K = 3.4 \times 10^{-4}\ ppb^{-1}$ are then extracted using (2) from the adsorption segment. Equilibrium surface coverage of the analyte ($\theta = KC_a/(1 + KC_a)$) can be predicted using a Langmuir isotherm. Finally, the Gibbs free energy of adsorption ($\Delta G_{ad} = -0.33$ eV), a thermodynamic potential related to the spontaneity of adsorption, and thus the reversibility, is estimated from (3). Note that a thermodynamic potential at equilibrium can be estimated from the transient sensor response. Considerable variation was observed from sensor to sensor, even for the same functionalization chemistry. The origins of this variation are discussed below.

$$\Delta G_{ad} = -RT \ln K \tag{3}$$

The average free energy values of −0.25, −0.30, and −0.16 eV are obtained in a similar way for ethylenediamine, pyridine, and hydrazine,[21] respectively (Figure 2g, diamond). These results suggest that the reversibility of SWNT sensor response can be tuned by systematically changing the surface chemistry. We also find that the values show a similar trend with the enthalpy of adsorption ($\Delta H_{ad,MP}$) between an amine and a thionyl chloride molecule estimated using a generic molecular potential (MP) calculation (Figure 2g, square). The results suggest the thionyl chloride binds directly to the amine-functionalization. The entropy change upon adsorption appears to be insignificant, which can be ascribed to the small size of thionyl chloride molecule. The estimated kinetic and thermodynamic parameters are summarized in Table 1.

We have found the exact conditions that influence the conversion from irreversible to reversible binding. Some amines

(19) Lee, C. Y.; Strano, M. S. *Langmuir* **2005**, *21*, 5192−5196.
(20) It should be noted that our model does not consider any diffusion barrier, and therefore the extracted parameters include diffusion factor, if there is any.
(21) Hydrazine-treated sensor showed unique responses. Only after ~8 s upon analyte removal did the signal start to recover. The recovery rate maximized at 10~20 s after the analyte removal (Supporting Information Figure S1). The mechanism is likely a surface reaction between hydrazine and thionyl chloride, or formation of a temporary charge transfer complex. Further study will answer this question.

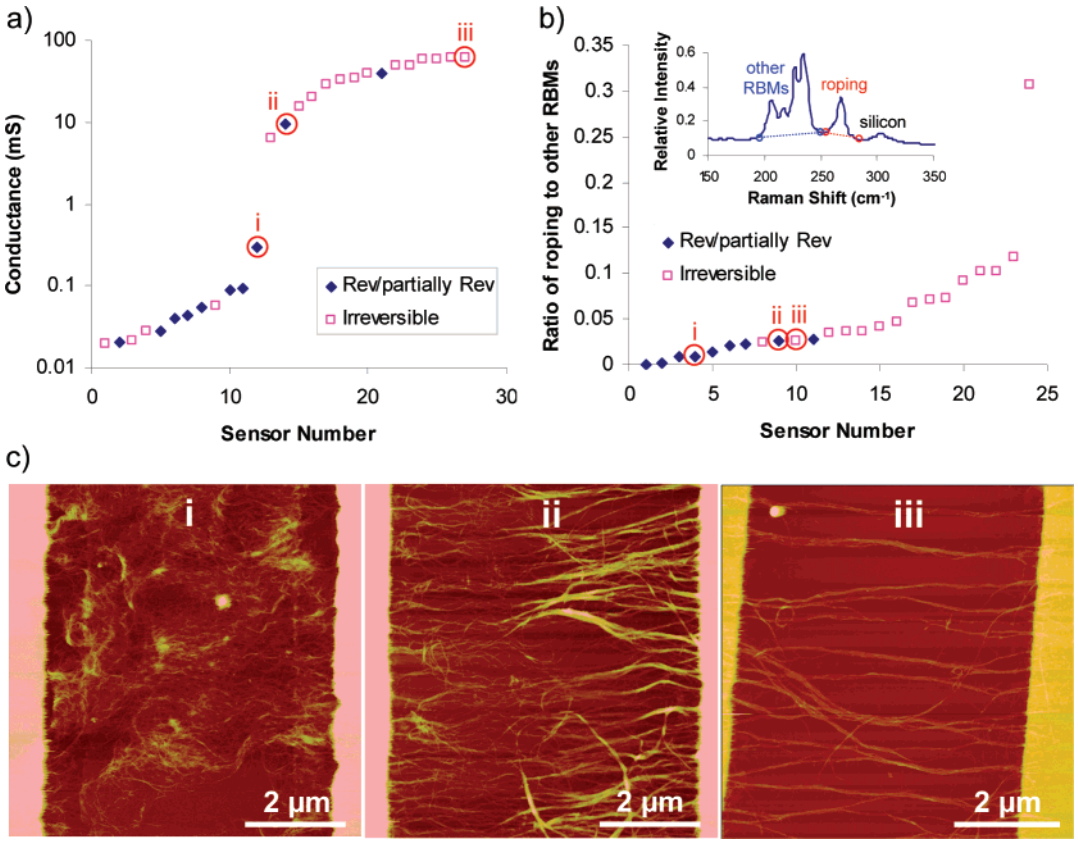

Figure 3. Required properties of SWNT network for effective functionalization. Array conductance and Raman features from 27 aniline-functionalized sensors are correlated with the reversibility. The diamonds and squares denote (partially) reversible and irreversible sensors, respectively. (a) Conductance versus reversibility, showing that a SWNT network near percolation threshold is desired. (b) Raman roping peak to other RBMs ratio versus reversibility. Minimal SWNT aggregation is necessary for the chemistry to effectively shift the reversibility. (c) AFM images from three representative sensor arrays i, ii, and iii from (a) and (b).

failed to produce reversible binding at all. Benzylamine, diethylenetriamine, dimethylamine, and triethylamine are among those that are not effective, meaning that the sensor response remained irreversible even after application of the chemistry. We also observe sensor to sensor variation, even for the same surface chemistry, for this irreversible to reversible conversion. This variability motivates an investigation of the exact conditions necessary for the change in adsorption mechanism. There is a strong correlation between the irreversible/reversible conversion, and a sub-percolated SWNT electronic network. We studied the conversion of 27 aniline-functionalized SWNT sensors to eliminate the chemistry as a variable. The functionalization is defined as effective if the response to a dilute thionyl chloride injection becomes (partially) reversible after treatment, and ineffective if it remains irreversible (Supporting Information Figure S2). The initial sensor conductance versus sensor number, assigned in ascending conductance order, is plotted as Figure 3a. We note that 67% of low conductance (<1 mS) sensors were reversible, whereas only 13% of high conductance (>1 mS) sensors were reversible. The trend displayed in Figure 3a is comparable with 2D percolation behavior in nanotube networks where a sharp conductance increase is observed well above percolation threshold.[22] We conclude that the SWNT network should be near or slightly above the percolation threshold for effective conversion.

The effect of nanotube aggregation on the effectiveness of chemical treatment was studied using Raman spectroscopy at 785-nm laser excitation. SWNT exhibit strong Raman scattering when the inter-band transition energy is in resonance with excitation laser, due to the unique van Hove singularities (vHs) in the density of states.[23] Each peak in the radial breathing mode (RBM) region of the spectrum is a vibrational mode in the radial direction that probes SWNT with a certain chirality vector (*n*,*m*) and electronic structure. A Raman peak at 267 cm^{-1}, i.e., the RBM of the (10,2) SWNT, becomes more prominent as nanotubes form electronically coupled aggregates and the interband transitions are subsequently broadened and shifted.[24] The ratio of this peak to other RBMs, shown as an inset, is a relative measure of inter-tube coupling or bundle size, and is also plotted versus sensor number in ascending order (Figure 3b). We find that nanotube aggregation state, probed spectroscopically in this manner, is a much more effective predictor of chemical effectiveness except for sensors 8 to 11 in the apparent transition region. AFM images support this correlation. Figure 3c shows the AFM images of three representative sensors. The first is a reversible sensor just near the onset of percolation (i), whereas (ii) is a reversible sensor just above percolation. Last, (iii) is an irreversible sensor far above percolation. It is apparent that (i) is composed mostly of individual or small bundles of nanotubes. Also, (ii) and (iii) have similar overall aggregation states but (ii) has more current

(22) Hu, L.; Hecht, D. S.; Gruner, G. *Nano Lett.* **2004**, *4*, 2513−2517.

(23) Dresselhaus, M. S.; Dresselhaus, G.; Avouris, P. *Carbon Nanotubes: Synthesis, Structure, Properties, and Applications*; Springer: Berlin; New York, 2001.

(24) Heller, D. A.; Barone, P. W.; Swanson, J. P.; Mayrhofer, R. M.; Strano, M. S. *J. Phys. Chem. B* **2004**, *108*, 6905−6909.

paths through individual nanotubes compared to (iii). It should be noted that for those that are sub-percolated and unbundled, the chemistry is effective 100% of the time.

Bundling can inhibit reversible binding by creating sites of much lower potential for adsorption than the SWNT sidewall. A SWNT bundle has four possible adsorption sites: the external surface, external groove, internal surface, and interstitial channel.[25] The external groove and interstitial channel are additional sites created upon bundling. Several studies[26,27] predict significantly higher binding energy for these adsorption sites. Our molecular potential (MP) calculations and XPS results (discussed in the next section) support the idea that the aniline could reduce the binding energy of thionyl chloride by irreversibly covering the entire SWNT surface. Aniline molecules will presumably functionalize a SWNT bundle along the equi-potential surface, which still has groove sites.[28] This could explain the chemistry failure for SWNT arrays with high aggregation states. This relationship between adsorption strength and array morphology explains the strong correlations of reversible behavior with sub-percolated networks, and low extent of bundling. We are the first to carefully examine the subtle nanoscale geometric and electrical variations that can ruin the otherwise effective chemistry. The variations will be greatly reduced as the nanotube field evolves in terms of controlled deposition/growth and separation by length and electronic structure.

In previous work,[10] we demonstrated that for a sparse SWNT network free from significant aggregation, the conductance change upon analyte adsorption increases linearly with the sensor conductance. A mass-action model of dynamic adsorption predicts this trend, which is due to the increase in surface area and binding sites for analyte adsorption. This assumes that each nanotube is an independent, isolated series of sites. However, when the array is dominated by large bundles, the behavior is different. Sensors with the highest current, corresponding to this regime, do not even respond to analyte. In this regime, the surface area to current ratio is the dominant factor. For sensors with large bundles, current pathways exist with no connection to surface sites. We observe this trend during aniline treatment as well. The percent conductance change after functionalization with aniline was inversely proportional to the array conductance, suggesting that aniline adsorbs primarily to external sites of SWNT bundles (Supporting Information Figure S3).

Thionyl chloride, a strong electron acceptor, is expected to adsorb more strongly on metallic SWNT than on semiconducting SWNT due to high electron-charge density at the Fermi level.[29] We performed in situ Raman spectroscopy to test this (Figure 4a). The conductance (black line) drops upon aniline addition and stabilizes (~1250 s) after aniline evaporation (Figure 4b). Subsequent thionyl chloride injections, 1000 ppm followed by 10 000 ppm, were made. Baseline-integrated RBM at 785 nm excitation, resonant only with semiconducting SWNT, was monitored in situ (blue line). Partial recovery was observed for both conductance and Raman signal, which changed in opposite direction to each other. This can be explained by increased hole carriers, and a decreased number of ground state electrons for photoabsorption upon electron-withdrawal by thionyl chloride. Raman spectroscopy at 632.8 nm excitation enables us to probe the effect of adsorption on metallic and semiconducting SWNT separately. Figure 4c shows baseline-integration of RBM, normalized by Si background peak, from aniline-functionalized metallic (green) and semiconducting (blue) nanotubes. Both types show partially irreversible decreases (conductance increase), seen in Figure 4b. The peak ratio of semiconducting to metallic SWNT is 0.71 initially, and 0.80 after thionyl chloride injection. We assigned this phenomena to the preferential charge transfer from metallic SWNT to thionyl chloride as discussed in our previous work.[10] However, the percent signal recovery after 10 min is 33% and 32% for semiconducting and metallic SWNT, respectively. We have therefore concluded that the desorption kinetics of thionyl chloride are indistinguishable with respect to SWNT electronic structure treated with aniline. Detailed change in the Raman spectra can be found in Supporting Information Figure S4.

Both small molecular weight and larger polymeric amines induce this conversion. The former can still have an n-doping effect on SWNT as documented for PEI functionalization.[6,12] Among 11 types of amine functionalities we have examined, only 4 turned out to effectively induce irreversible to reversible transition as shown in Figure 2b−e. Conversely, for the ineffective amines the responses remained either irreversible or indefinable (Supporting Information Figure S5). The primary *y*-axis in Figure 4d shows pK_a values for ineffective (filled red) and effective (filled blue) amine functionalities. Only amines below pK_a of 8.8 are apparently effective, suggesting a correlation with basicity. We first hypothesized that the change in reversibility was due to doping by the amine. In this scenario, amine molecules fill groove sites on SWNT bundles, leaving the external surface available for analyte adsorption. The increase in SWNT Fermi level by amines, however, would increase the SWNT−$SOCl_2$ binding energy. Hence, we abandon this hypothesis.

Molecular potential (MP) calculations were carried out on a (10,0) SWNT to understand the aniline interaction. Irreversible binding of thionyl chloride on a (10,0) SWNT does so with an energy (E_b) of −0.367 eV. The higher binding energy for an aniline molecule (E_b = −0.564 eV) predicts that aniline irreversibly adsorbs on SWNT surfaces. The array conductance decreased permanently upon aniline addition, and the presence of strongly bound aniline after evaporation was confirmed in X-ray photoelectron spectroscopy (XPS). Average atomic N/C ratio was 1.76 ± 1.61% and 6.74 ± 3.23% for 3 untreated and 11 aniline-functionalized sensors, respectively. Price and Tour[30] recently reported SWNT functionalization with substituted anilines at 80 °C for 12 h in the presence of oxidizing agents, but we do not expect this reaction to occur in the milder conditions of our system. No noticeable increase in D-peak, a Raman signature of covalent functionalization of SWNT, was observed after aniline treatment. Monolayer aniline coverage predicted by MP corresponds to 27 aniline molecules for a 6.5 unit cell (10,0) SWNT. The estimated N/C ratio is 6.11%, which is lower than 6.74% in XPS. These results support that aniline irreversibly adsorbs upon the entire SWNT surface so that no bare SWNT surface is exposed for analyte adsorption.

(25) Shi, W.; Johnson, J. K. *Phys. Rev. Lett.* **2003**, *91*, 015504.
(26) Bienfait, M.; Zeppenfeld, P.; Dupont-Pavlovsky, N.; Muris, M.; Johnson, M. R.; Wilson, T.; DePies, M.; Vilches, O. E. *Phys. Rev. B* **2004**, *70*, 035410.
(27) Zambano, A. J.; Talapatra, S.; Migone, A. D. *Phys. Rev. B* **2001**, *64*, 075415.
(28) Jiang, J. W.; Sandler, S. I. *Phys. Rev. B* **2003**, *68*, 245412.
(29) Seo, K.; Park, K. A.; Kim, C.; Han, S.; Kim, B.; Lee, Y. H. *J. Am. Chem. Soc.* **2005**, *127*, 15724−15729.
(30) Price, B. K.; Tour, J. M. *J. Am. Chem. Soc.* **2006**, *128*, 12899−12904.

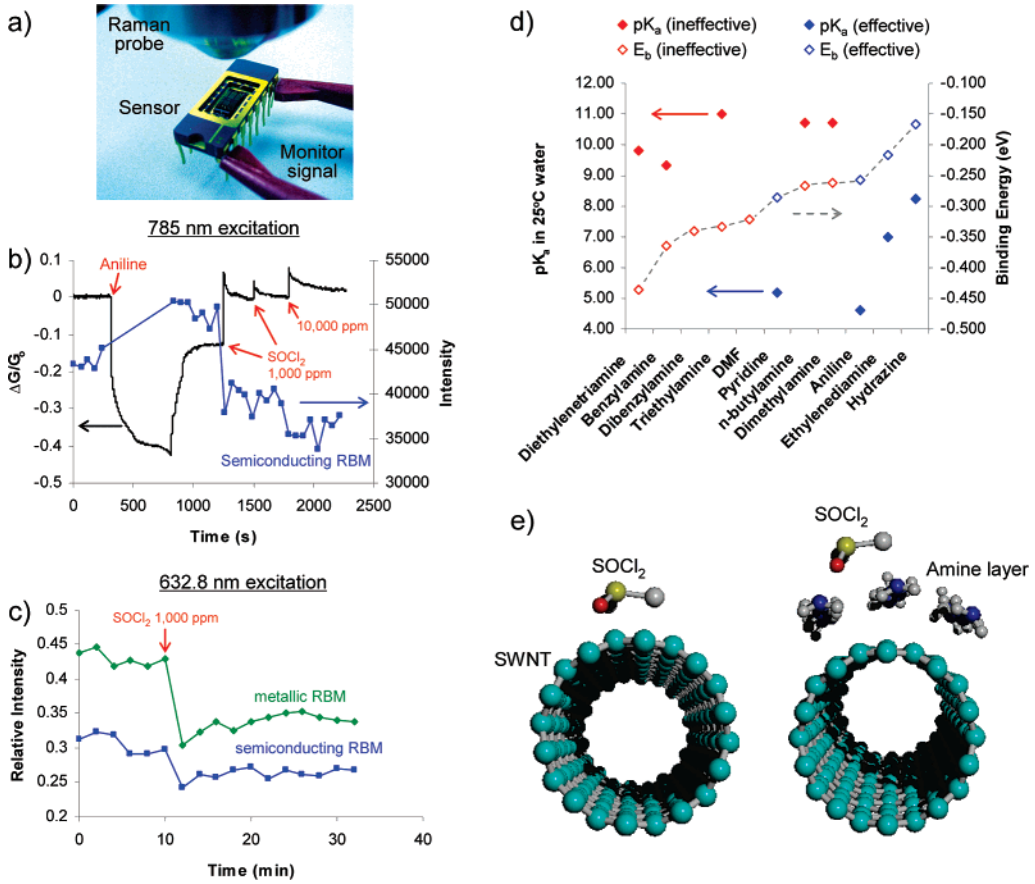

Figure 4. Proposed mechanism for tuned reversibility. **(**a) Picture showing in situ Raman on aniline-treated sensor exposed to thionyl chloride. (b) Baseline-integrated RBM (blue) from semiconducting nanotubes at 785-nm laser excitation, monitored in situ with conductance (black). Irreversible conductance decrease corresponds to irreversible increase in Raman signal. (c) Real-time Raman at 632.8 nm laser excitation. Desorption kinetics of thionyl chloride does not differ between metallic (green) and semiconducting (blue) nanotubes. (d) pK_a of amine molecules tested, and the binding energy (E_b) between a thionyl chloride and a amine molecule calculated by molecular potential. Red and blue shapes represent ineffective and effective functionalization, respectively. Filled and open shapes correspond to pK_a on the primary axis and E_b on the secondary axis, respectively. Effective surface chemistry reduces the thionyl chloride binding energy, causing reversible responses. (e) Thionyl chloride adsorbed on a bare SWNT (left), and on a functionalized SWNT (right).

Hence, thionyl chloride is expected to adsorb on the amine layer rather than on SWNT surface as illustrated in Figure 4e. The binding energy of thionyl chloride-amine complex was estimated using MP calculations for 10 different amines (Figure 4d, secondary *y*-axis, open shapes). No SWNT was involved in this calculation. The calculated E_b values were smaller for effective amines (blue) than for ineffective ones (red). Therefore we propose that amine functionalization reduces the thionyl chloride binding energy, resulting in reversible sensor responses. The amine layer in this system acts as a mediator for charge transfer from SWNT to thionyl chloride.

The possibility of a reaction between thionyl chloride and amine molecules was considered. It is well-known that thionyl chloride readily reacts with amines under some conditions.[31,32] The expected reaction products with aniline are *N*-sulfinyl-benzenamine and HCl.[33] Reduction of thionyl chloride could also occur to form SO_2, S, and Cl^-.[34,35] Either case would affect the sensor signal by producing strongly bound reaction products or removing the amine layer. The MP calculations predict the E_b of *N*-sulfinyl-benzenamine, HCl, and SO_2 on (10,0) SWNT would be −0.669, −0.139, and −0.300 eV, respectively. The strongly binding *N*-sulfinyl-benzenamine would especially cause an irreversible sensor response. Therefore, the stable baseline in Figure 2b suggests that these possibilities can be rejected. There was also no residual sulfur evident via XPS from aniline-treated sensors exposed to thionyl chloride. This further supports the absence of the reaction (Supporting Information Figure S6). We speculate that this is due to the reduced basicity and reactivity of amines that have partial electron donation to the SWNT.[36] Conversely, ineffective amine treatments in Figure 4d, which are categorically stronger bases than those of the effective group, potentially react with thionyl chloride and form irreversibly binding species. Thionyl chloride in our system appears to functionally behave similarly to SO_2 molecules for probing the surface basicity.[37,38]

If the amine moiety represents the new, reversible binding site, intermediate to the SWNT array, then a polymeric form should increase the detection limit of the system by increasing the number of sites per area. We find that the sensitivity to thionyl chloride was dramatically improved by polyethylene-

(31) Arrieta, A.; Aizpurua, J. M.; Palomo, C. *Tetrahedron Lett.* **1984**, *25*, 3365−3368.
(32) El-Sakka, I. A.; Hassan, N. A. *J. Sulfur Chem.* **2005**, *26*, 33−97.
(33) Ghosh, M. *Polym. Bull.* **1988**, *19*, 1−6.
(34) Bernstein, P. A.; Lever, A. B. P. *Inorg. Chem.* **1995**, *34*, 933−937.
(35) Dampier, F. W.; Cole, T. A. *J. Electrochem. Soc.* **1987**, *134*, 2383−2387.
(36) Luo, N.; Stewart, M. J.; Hirt, D. E.; Husson, S. M.; Schwark, D. W. *J. Appl. Polym. Sci.* **2004**, *92*, 1688−1694.
(37) Waqif, M.; Saad, A. M.; Bensitel, M.; Bachelier, J.; Saur, O.; Lavalley, J. C. *J. Chem. Soc., Faraday Trans.* **1992**, *88*, 2931−2936.
(38) Morenocastilla, C.; Carrascomarin, F.; Utrerahidalgo, E.; Riverautrilla, J. *Langmuir* **1993**, *9*, 1378−1383.

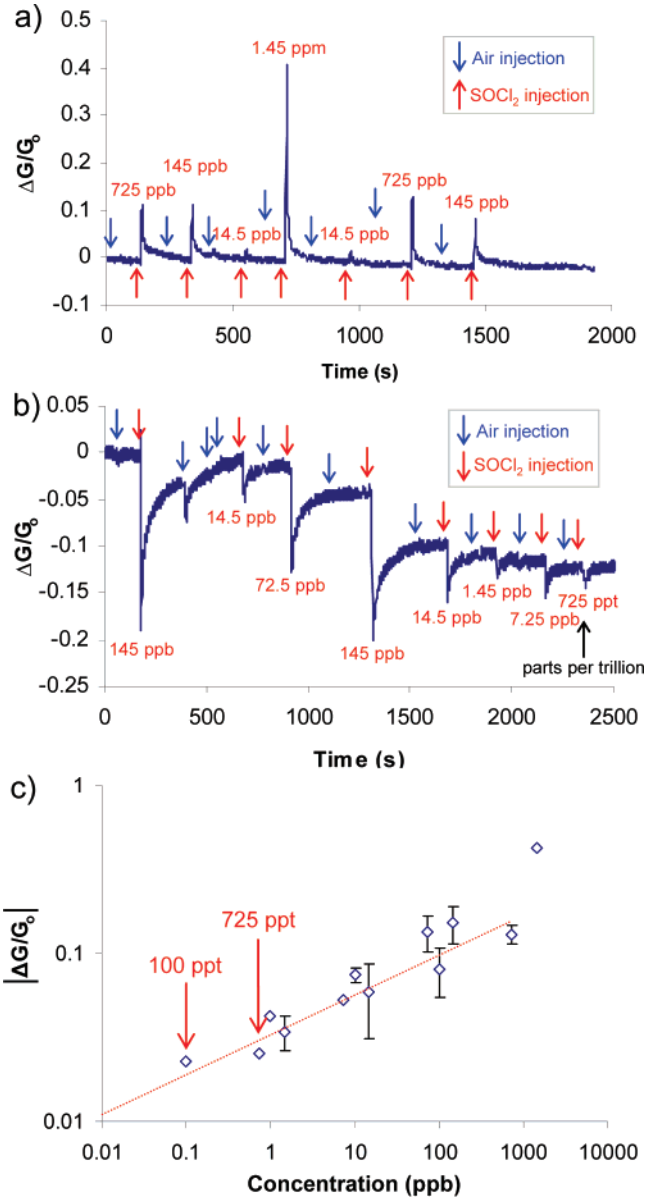

Figure 5. Enhanced sensitivity via polymer functionalization. Sensor response to thionyl chloride can be dramatically improved by PEI functionalization without loosing the reversibility. (a) Positive responses to thionyl chloride. (b) Negative responses to thionyl chloride showing ppt level detection. (c) Response curve from 5 PEI-treated sensors. The estimated detection limit, at 3× the noise level, is 25 ppt.

imine (PEI) functionalization (Figure 5a). Red and blue arrows denote thionyl chloride and air injections, respectively. A sharp signal increase was observed even at the ppb level, and the response was reversible with stable baseline. Regular air injections (as shown) were made to monitor any potential contamination in the injection system or background. Negative responses were observed from another sensor (Figure 5b). Each response meets our reversibility criterion of $t_{1/2} < 60$ s. However, it is noted that the sensor cannot be identified as completely reversible since slight baseline drifts from each accrue. The origin of this irreversible component is discussed earlier. A parts-per-trillion (ppt) level detection for an irreversible system was demonstrated by Qi et al.[6] where the analyte accumulation over time is eventually transduced into sensor response. We were able to detect a 5-s pulse of 10 mL thionyl chloride at 725 ppt

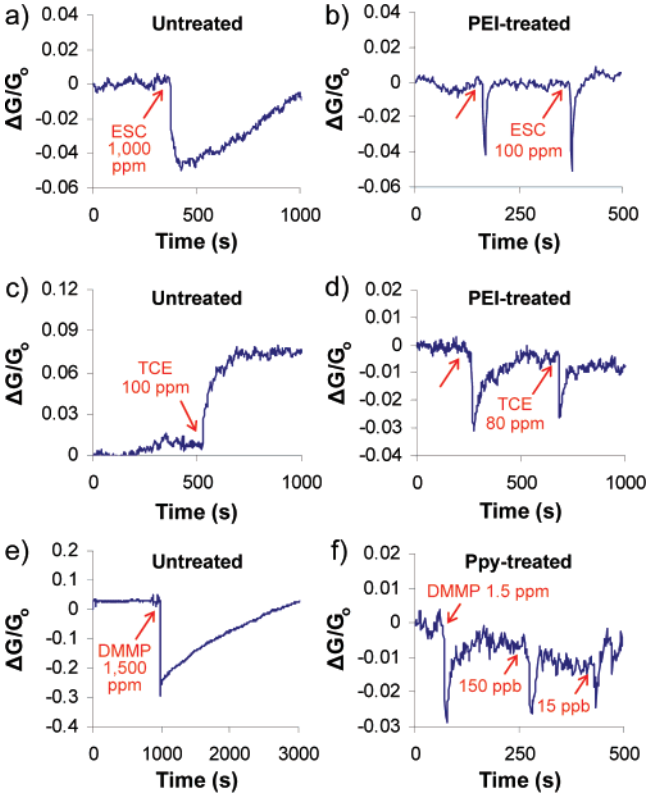

Figure 6. Irreversible-to-reversible transition from other systems. The transition via surface chemistry is shown to be generic. (a) Irreversible response ($t_{1/2} = 345$ s) to ethanesulfonyl chloride (ESC) from untreated sensor. (b) Reversible detection of ESC using PEI-treated sensor. (c) Irreversible response to 1,1,2,2-tetrachloroethane (TCE) without any treatment. (d) Reversible TCE response from PEI-treated sensor. (e) Irreversible response ($t_{1/2} = 570$ s) to dimethyl methylphosphonate (DMMP) from untreated sensor made by membrane transfer technique. (f) Reversible DMMP response from polypyrrole (Ppy)-treated membrane transfer sensor.

(parts per trillion), which is the lowest concentration to date detected reversibly by a SWNT sensor. We believe the sign of the signal is related to the extent of n-doping by PEI. Electron withdrawal by thionyl chloride from an n-type (p-type) array will cause a decrease (increase) in conductance by removing (introducing) the majority carriers. Figure 5c is a response curve from 5 representative PEI-treated sensors. The lowest detection limit, extrapolated to three times the noise level, is 25 ppt. This enhancement in sensitivity of over 3 orders of magnitude is also due in part by the Fermi level increase due to PEI doping, up to the most probable first vHs in conduction band (~0.516 eV from mid-gap for HiPco[39]).

The irreversible-to-reversible transition upon surface functionalization is not limited only to thionyl chloride but a general phenomenon. Figure 6a shows an irreversible response with $t_{1/2} = 345$ s to 1000 ppm ethanesulfonyl chloride (ESC) vapor from an untreated array. Upon functionalization with PEI the response became reversible with an order of magnitude increase in sensitivity (Figure 6b). A similar transition after PEI treatment, but without sensitivity improvement, was observed for the detection of 1,1,2,2-tetrachloroethane (TCE) (Figure 6c−d). We were also able to observe this transition in a completely different system. An electronic sensor array, consisting of a random network of laser ablation SWNT, was prepared via membrane-

(39) Kukovecz, A.; Kramberger, C.; Georgakilas, V.; Prato, M.; Kuzmany, H. *Eur. Phys. J. B* **2002**, *28*, 223−230.

transfer.[40] This type of array has more nanotube−nanotube junctions than the dielectrophoretically formed aligned network. A different nanotube diameter distribution, and thus chirality and work function, further alters the array properties. The analyte tested was dimethyl methylphosphonate (DMMP), a nerve agent simulant. The untreated array was insensitive at ppb to low ppm level. The 1500 ppm response from untreated sensor was irreversible with $t_{1/2} = 570$ s (Figure 6e), whereas polypyrrole (Ppy)-treated sensor responds reversibly at ppb level (Figure 6f). The results suggest that our approach of reducing the analyte binding energy via surface chemistry is generic and can be extended to other systems.

We have demonstrated the reversibility of SWNT gas sensor can be tuned by variation of the surface chemistry. Kinetic and thermodynamic parameters extracted from the reversible responses match calculated binding energy between analyte and surface functional group. It is shown that irreversibly bound amine layers below pK_a of 8.8 reduce the analyte binding energy. The absence of strong adsorption sites, such as grooves in a SWNT bundle, is a prerequisite for the amine functionalization to effectively reduce the analyte binding energy. Providing more adsorption sites by PEI functionalization enables both reversibility and ppt-level sensitivity to thionyl chloride. We have shown this irreversible-to-reversible transition from several systems and concluded that it is a general phenomenon.

3. Methods

3.1. Sensor Fabrication. 3.1.1. Dielectrophoresis Sensors. Interdigitated gold electrodes with 5 μm gap were patterned on a thermally oxidized Si wafer (600 nm SiO_2, Montco Silicon Technologies) by photolithography. The electrodes mounted on a chip carrier were wire-bonded for electrical connection. HiPco SWNT (batch HPR 107.1) was suspended in 1 wt % sodium dodecyl sulfate (SDS) aqueous solution by 10 min sonication, followed by 4 h centrifugation at 30 000 RPM. AC-dielectrophoresis was performed to form a SWNT network. AC voltage (10 V_{pp}, 5 MHz) was applied across the electrodes, and ~1 μL of SWNT solution was dropped onto the electrodes. SWNT coverage was roughly controlled by deposition time. After shutting off the power the substrate was rinsed with 1 wt % SDS solution and DI water to remove residual SDS.

3.1.2. Membrane Ttransfer Sensors. SWNT grown by laser ablation, individually suspended in 2 wt % sodium cholate aqueous solution, were filtered through a mixed cellulose ester membrane (Millipore) with 25 nm pores. SWNT on the membrane were transferred to a silicon substrate, followed by patterning the interdigitated electrodes as above. Nanotubes outside the active sensing area were then removed by reactive ion etching. Details of the membrane transfer technique can be found in Wu et al.[40]

3.2. Sensor Functionalization and Testing. 3.2.1. Non-polymeric Amine Functionalization. A 1 μL portion of aniline (Acros) was applied onto the sensor, followed by removal of excess liquid aniline after 3 min. The remaining aniline was evaporated, and the signal was stabilized before testing. All other non-polymeric amines were functionalized in a similar way.

3.2.2. PEI Functionalization. PEI (Aldrich, M_n~423) was dropped onto the sensor and blown with ~15 psi N_2 stream. This forms a ~10 μm wet PEI film.

3.2.3. Ppy Functionalization. The sensor was wetted with 5 wt % Ppy aqueous solution (Aldrich) for 2 min and rinsed with DI water.

3.2.4. Testing. Saturated analyte vapor was diluted in series for desired concentration. A pulse of 10-mL analyte (~2 mL/s) vapor at desired concentration was flown onto the sensors with non-polymeric amines, PEI, or Ppy layers. Injections were made using a glass syringe to prevent corrosion and contamination. The array conductance was monitored at 1 mV. All functionalization and testings were performed at room temperature air.

3.3. MP Calculations. Molecular potential calculations were performed using universal force field (UFF)[41] and Gasteiger charge calculation[42] in a Cerius2 program.[43] We assumed the molecular geometry of deposited SWNT and amine molecules did not change in response to the analyte adsorption. For the bindings on SWNT, a 6.5-unit cell (10,0) SWNT was first optimized, and the energy of analyte or amine molecules was minimized with the SWNT fixed. For the amine−analyte interaction (Figure 4d), an amine molecule was optimized, followed by energy minimization of thionyl chloride with the amine molecule immobilized. Different initial orientations were considered to find the global minima. The binding energy (E_b) of molecule A on molecule B was defined as the amount of energy reduced by adsorption (i.e., $E_{b,A} = E_A$(adsorbed on B) $- E_A$(free)).

Acknowledgment. This work was supported by the Department of Homeland Security and the Federal Aviation Administration under Grant No. DHS S&T 06-G-026. AFM and XPS analysis were carried out in the Center for Microanalysis of Materials, University of Illinois, which is partially supported by the U.S. Department of Energy under Grant No. DEFG02-91-ER45439. The authors thank R. Sharma for useful discussions, R. T. Haasch for XPS measurements, and J. Y. Baudry for help with MP calculations. Laser ablation nanotubes from F. Henrich and M. M. Kappes at the University of Karlsruhe are also acknowledged.

Supporting Information Available: Unique desorption kinetics of thionyl chloride from hydrazine-treated sensors; example responses to thionyl chloride from aniline-treated sensors (effective versus ineffective); reduced sensitivity for large bundles; changes in Raman spectra upon chemical treatment; examples of ineffective amine functionalities; S 2p peak in XPS from untreated and aniline-treated sensors after exposure to thionyl chloride. This material is available free of charge via the Internet at http://pubs.acs.org.

JA0776069

(40) Wu, Z. C.; Chen, Z. H.; Du, X.; Logan, J. M.; Sippel, J.; Nikolou, M.; Kamaras, K.; Reynolds, J. R.; Tanner, D. B.; Hebard, A. F.; Rinzler, A. G. *Science* **2004**, *305*, 1273−1276.
(41) Rappe, A. K.; Casewit, C. J.; Colwell, K. S.; Goddard, W. A.; Skiff, W. M. *J. Am. Chem. Soc.* **1992**, *114*, 10024−10035.
(42) Gasteiger, J.; Marsili, M. *Tetrahedron* **1980**, *36*, 3219−3228.
(43) Accelry http://www.accelrys.com/products/cerius2/.